Salinity of the Eocene Arctic Ocean from oxygen isotope analysis of fish bone carbonate

Lindsey M. Waddell[1] and Theodore C. Moore[1]

Received 12 March 2007; revised 27 November 2007; accepted 10 January 2008; published 22 March 2008.

[1] Stable isotope analysis was performed on the structural carbonate of fish bone apatite from early and early middle Eocene samples (~55 to ~45 Ma) recently recovered from the Lomonosov Ridge by Integrated Ocean Drilling Program Expedition 302 (the Arctic Coring Expedition). The $\delta^{18}O$ values of the Eocene samples ranged from −6.84‰ to −2.96‰ Vienna Peedee belemnite, with a mean value of −4.89‰, compared to 2.77‰ for a Miocene sample in the overlying section. An average salinity of 21 to 25‰ was calculated for the Eocene Arctic, compared to 35‰ for the Miocene, with lower salinities during the Paleocene Eocene thermal maximum, the *Azolla* event at ~48.7 Ma, and a third previously unidentified event at ~47.6 Ma. At the *Azolla* event, where the organic carbon content of the sediment reaches a maximum, a positive $\delta^{13}C$ excursion was observed, indicating unusually high productivity in the surface waters.

Citation: Waddell, L. M., and T. C. Moore (2008), Salinity of the Eocene Arctic Ocean from oxygen isotope analysis of fish bone carbonate, *Paleoceanography*, *23*, PA1S12, doi:10.1029/2007PA001451.

1. Introduction

[2] The Arctic is relatively isolated from the world ocean and receives a net surplus of freshwater through the hydrologic cycle, mostly as runoff. The freshwater surplus creates a low-salinity layer (32.5‰) in the upper 50 m of the Arctic water column, known as the Polar Mixed Layer, which limits vertical mixing and promotes sea ice formation. As a result, the Arctic exhibits a strong salinity stratification and an estuarine-like circulation pattern, with the lighter, fresher waters of the Polar Mixed Layer overriding Atlantic waters entering through the Fram Strait. Low-salinity surface water is exported to the Norwegian-Greenland Sea via the East Greenland Current, where it mixes with relatively warm, saline water from the Atlantic and sets up the deep convection that produces the Denmark Strait Overflow Water (DSOW) and the Iceland Sea Overflow Water (ISOW), the densest components of North Atlantic Deep Water (NADW), which enter the Atlantic basin through overflow of the Greenland-Faroe Ridge. The Arctic plays a vital role in global climate through its influence on the production of NADW. However, deepwater formation in the Norwegian-Greenland Sea is delicately balanced, and an increase in the export of fresh water from the Arctic, whether through a reduction in surface salinity or an increase in sea ice discharge, has the potential to cap convective regions and reduce thermohaline circulation [*Aagaard and Carmack*, 1989]. An example of such an event is the "Great Salinity Anomaly" of the late 1960s. During this time a freshening of the surface waters north of Iceland may have resulted from a 25% greater than average outflow of fresh water from the Arctic Ocean over a 2 year period [*Aagaard and Carmack*, 1989]. The anomaly corresponded with a significant freshening and cooling of North Atlantic Deepwater [*Brewer et al.*, 1983], and its occurrence raises concerns about the threat the Arctic could pose to NADW formation under future anthropogenic warming.

[3] During the greenhouse climate of the early and mid Eocene, plate tectonic reconstructions suggest that the Arctic may have had even less of a deepwater connection to the world ocean than it does today (Figure 1). Without major continental ice sheets at this time, sea level was substantially (30–100 m) higher than in modern times [*Miller et al.*, 2005a]; however the Fram Strait, the only deep connection between the Arctic and the world ocean, may not have allowed for bidirectional exchange with the Norwegian-Greenland Sea until 17.5 Ma [*Jakobsson et al.*, 2007] and may not have opened fully until the late Miocene [*Lawver et al.*, 1990]. Thus with an intensified hydrologic cycle under a warm Eocene climate and fewer connections to the world ocean, it might be expected that the near surface water of the Eocene Arctic was even fresher than it is today and that the outflow of low-salinity water from the basin may have acted to prevent the formation of deepwater in the high-latitude northern seas.

[4] Recent evidence suggests significant shifts in deepwater and intermediate-water production between the high southern and high northern latitudes in response to changes in global temperature during the late Cretaceous and Paleogene. As the highest-latitude ocean basin, the exact role of the Arctic in deep water production during this period is still uncertain. Modeling studies and $\delta^{13}C$ data suggest that a significant intensification of the hydrologic cycle in response to extreme global warmth may have initiated a switch in deepwater formation from the high southern to the high northern latitudes [*Bice and Marotzke*, 2002; *Nunes and Norris*, 2006]. During peak warmth, the salinity of Southern Ocean surface waters would have been signifi-

[1]Department of Geological Sciences, University of Michigan, Ann Arbor, Michigan, USA.

0883-8305/08/2007PA001451

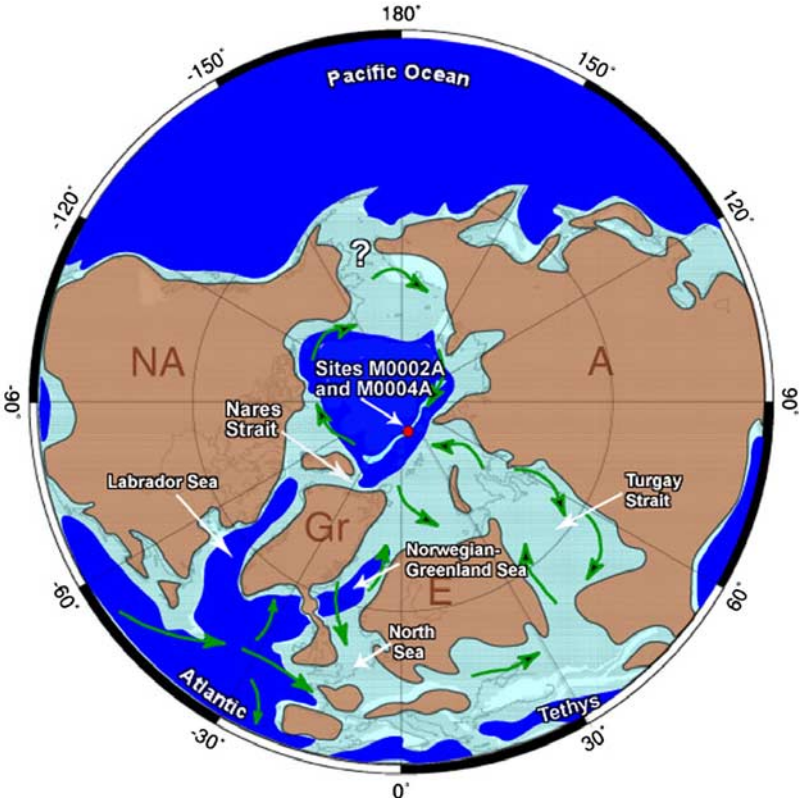

Figure 1. Paleoreconstruction of the Arctic region at 50 Ma showing the location of the Arctic Coring Expedition (ACEX) 302 sites examined in this study. Modified from the *Expedition 302 Scientists* [2006].

cantly reduced by an increase in high-latitude precipitation, thereby inhibiting convection, but deepwater formation in the North Pacific may have been enhanced by the import of higher-salinity subtropical surface waters from the North Atlantic through the Central American Seaway. In the modeling studies of *Bice and Marotzke* [2002], deep convection occurs in the high northern latitudes at the PETM despite an intensified hydrologic cycle because Arctic outflow is diverted directly into the northwestern Tethys by the Greenland-Faroe Ridge. Uplift of the North Atlantic region may have severed the Rockall Trough connection between the Atlantic and Arctic and allowed mammal migration between North America and Europe across the Greenland-Faroe Ridge over an approximately 2 Ma period in the late Paleocene and early Eocene [*Knox*, 1998]. However, once a surface water connection was reestablished between the Arctic and the North Atlantic, we must be concerned with the possible role of Arctic outflow on oceanic circulation.

[5] To better evaluate oceanographic conditions within the Arctic basin, and thus the possible impact of Arctic outflow on global circulation, this study estimates the salinity of the Eocene Arctic Ocean using $\delta^{18}O_{CO3}{}^{2-}$ of fish apatite from cores recently recovered from the Lomonosov Ridge by Integrated Ocean Drilling Program (IODP) Expedition 302, the Arctic Coring Expedition (ACEX). The results of this study will also allow an assessment of the degree of isolation of the Arctic Ocean during the Eocene.

2. Tectonic Setting

[6] The modern Arctic Ocean contains two deep basins separated by the Lomonosov Ridge: the Amerasia and Eurasia Basins. The Amerasia Basin, in turn, is divided into two subbasins, the Canada and Makarov, by the Alpha-Mendeleev Ridge, and the Eurasia Basin is divided into the Nansen and Amundsen subbasins by the Gakkel Ridge, the Arctic crustal spreading center. Although the tectonic evolution of the Eurasia Basin is much better understood than that of the Amerasia Basin, it is commonly accepted that the Canada subbasin of the Amerasia Basin opened in the early Cretaceous through seafloor spreading along a now extinct ridge. The spreading resulted in the counterclockwise rotation of the Arctic Alaska and Chukotka terranes away from the Arctic Islands and toward their respective present-day locations in northern Alaska and Siberia [*Lawver et al.*, 2002]. By the mid Cretaceous, circulation between the Arctic and Pacific had been obstructed by the rotated blocks [*Johnson et al.*, 1994], and by the late Cretaceous, the Arctic connection to the Pacific Ocean was probably closed as mammals were able to migrate between Asia and western North America via the Beringia land bridge [*Averianov and Archibald*, 2003]. The complicated arrangement of microplates in easternmost Siberia, however, leaves some doubt

about the exact nature of interbasin passages between the Arctic and the Pacific during the early Cenozoic.

[7] Spreading in the Eurasia basin along the Gakkel Ridge commenced between Anomaly 24 and 25 (~57 Ma), close to the Paleocene/Eocene boundary and approximately contemporaneous with the onset of spreading in the southern Norwegian-Greenland Sea [*Thiede and Myhre*, 1996]. It is widely accepted that the Lomonosov Ridge is of continental origin and was rifted as a series of tilted fault blocks from the Barents/Kara Shelf during the opening of the Eurasia Basin [*Johnson et al.*, 1994]. Since rifting, the ridge has subsided to modern depths of approximately 1000–1600 m and has posed a great barrier to deep circulation within the Arctic since its creation [*Johnson et al.*, 1994].

[8] Reconstructions show no clear evidence of a deepwater connection between the Arctic and the world ocean during the Eocene. The opening of the Norwegian-Greenland Sea between Greenland and Svalbard was delayed until Anomaly 13, so the Fram Strait, the only deepwater connection between the Arctic and Norwegian Greenland Sea in existence today, may have allowed only shallow water exchange prior to the early Miocene (17.5 Ma) [*Jakobsson et al.*, 2007], with a full opening and deepwater exchange existing at least since the late Miocene (7.5 to 5 Ma) [*Lawver et al.*, 1990]. Also, according to simple thermal subsidence models, the Greenland-Faroe Ridge, an area of anomalously thick crust extending across Iceland from Greenland to the Faroes, likely prevented significant deep water overflow from the Norwegian-Greenland Sea to the North Atlantic until at least the early Miocene (~17 Ma) [*Wright*, 1998].

[9] There is evidence to support the existence of shallow water connections between the Arctic and the world ocean during the Eocene, but some of these connections may have been intermittent. Sea level was much higher in the Eocene than today because of the absence of large continental ice sheets, but studies of sequence stratigraphy along continental margins have suggested that sea level fluctuations of approximately 20–30 m were superimposed on the high sea levels of the late Cretaceous-Eocene [*Miller et al.*, 2005b]. Specifically, hiatuses/sequence boundaries on the New Jersey platform indicate significant sea level lowerings during the early middle Eocene at ~49 Ma, ~48 Ma, and ~46.2 Ma, and at ~42.6 and ~40.2 Ma in the late middle Eocene [*Miller et al.*, 2005b]. *Miller et al.* [2005b] have used benthic foraminiferal $\delta^{18}O$ to link these Cretaceous-Eocene sea level fluctuations to the existence of ephemeral ice sheets on Antarctica. Although oxygen isotope analyses of exceptionally well-preserved foraminifera from the Demerara Rise have challenged the existence of ice sheets during the Cretaceous [*Moriya et al.*, 2007], the existence of small ice sheets on Antarctica during the middle Eocene remains a possibility.

[10] Shallow water connections between the Arctic and the world ocean during the Eocene included the Turgay Strait and a seaway extending into the North Sea Basin [*Marincovich et al.*, 1990]. According to *Iakovleva et al.* [2001], the Turgay Strait probably did not provide a complete connection between the Arctic and Tethys during the Paleocene because dinocyst species of clear Tethyan affinity are not present in the flood deposits of the Sokolovsky Quarry of Kazakhstan. *Radionova and Khokhlova* [2000], however, have correlated thick Ypressian diatomite units extending from the Kara Sea to the north Turgay region to siliceous sediments in the North Atlantic Ocean, providing evidence for a connection between the North Atlantic and Tethys through the Arctic and Turgay Strait during the early Eocene. By the earliest middle Eocene, however, the connection between the Arctic and the West Siberian basin had apparently ceased to exist [*Radionova and Khokhlova*, 2000]. Shallow water exchange between the Atlantic and Arctic Oceans through the Labrador Sea and Baffin Bay may have developed as early as the Campanian-Maastrichtian [*Gradstein and Srivastava*, 1980], but the connection was always small. The convergence of Ellesmere Island and northwestern Greenland in the early Cenozoic further lessened the possibility of significant exchange through this passageway through the narrowing of the Nares Strait [*Srivastava*, 1985].

3. Results From Previous Work

[11] Vertebrate fauna recovered from Ellesmere Island in the 1970s provided some of the first evidence that temperatures in the early Eocene Arctic were substantially warmer than today. The discovery of early Eocene remains of the varanid lizard, the tortoise *Geochelone*, and the alligator *Allognathosuchus* suggested an Arctic climate similar to that of the southeastern United States today, with winter temperatures that rarely dipped below freezing [*Estes and Hutchinson*, 1980]. Isotopic analysis of cellulose from *Metasequoia* wood recovered at 80°N on Axel Heiberg Island indicates that the Arctic climate was not only warm (mean annual temperature (MAT) of 13.2 ± 2.0°C), but also quite humid during the middle Eocene, with an atmospheric water content approximately twice that of today [*Jahren and Sternberg*, 2003].

[12] Global compilations of $\delta^{18}O$ measurements on deep-sea benthic foraminifera have resolved the middle part of the early Eocene (52 to 50 Ma) as the warmest period of the Cenozoic; the exceptional warmth was the culmination of a pronounced warming trend spanning the mid-Paleocene to the early Eocene and was followed by a 17 Ma trend toward cooler conditions [*Zachos et al.*, 2001]. Embedded within the warming trend was the probable the release of 2000–4000 Gt of carbon from methane hydrates over a period of a thousand years at the PETM (55 Ma) [*Dickens*, 1999]. Increased atmospheric CO_2 levels in the early Eocene would have intensified the hydrologic cycle, resulting in increased subtropical evaporation and increased high-latitude precipitation [*Manabe*, 1997]. Because climatic conditions were humid [*Jahren and Sternberg*, 2003], continental freshwater drainage into the Arctic remained substantial, and the Greenland-Faroe Ridge prevented exchange with the North Atlantic, there is reason to believe that the waters of the Arctic and the Norwegian Greenland Sea may have been brackish during the early Eocene. Prior to the recent drilling expedition to the Lomonosov Ridge, the only existing Arctic deep-sea core of Paleogene age was

the mid-Eocene USGS Core Fl-422 from the Alpha Ridge, which measured only 364 cm in length and did not provide a clear indication of Arctic paleosalinity. *Clark and Kitchell* [1979] believed that the assemblage of diatom and silicoflagellates in Fl-422 was typical of normal marine conditions during the Paleocene, but *Bukry* [1984] asserted that the silicoflagellates were representative of an unusual assemblage of Eocene, rather than Paleocene, age. A follow-up study by *Magavern et al.* [1996] using $^{87}Sr/^{86}Sr$ ratios of fish bones and teeth from Fl-422 yielded $^{87}Sr/^{86}Sr$ values significantly higher than those of the world ocean at the time [*Burke et al.*, 1982], but considerable variability in values obtained from the same sample interval led *Magavern et al.* [1996] to attribute the high $^{87}Sr/^{86}Sr$ values to diagenetic alteration rather than to low-salinity conditions in an isolated, runoff-dominated basin.

[13] In a study of $\delta^{18}O_{CO3}{}^{2-}$ of fish apatite from ODP Leg 151 Hole 913B in the Norwegian-Greenland Sea, *Andreasson et al.* [1996] found indications that the Greenland Basin was brackish (estimated 22 to 28‰) during the early Eocene. With a humid climate and a weak connection between the Greenland Basin and the North Atlantic, there is a strong possibility that brackish conditions may also have existed throughout the Norwegian-Greenland Sea and the Arctic.

4. Summary of ACEX Findings

[14] Thorough investigation of the paleosalinity of the Arctic has been awaiting the acquisition of the first long, continuous, deep-sea sediment cores from the region. In the summer of 2004, the IODP Expedition 302, Arctic Coring Expedition (ACEX), successfully recovered ~340 m of sediments from the Lomonosov Ridge over a total depth of 428 mbsf [*Expedition 302 Scientists*, 2005]. The recovered material ranges in age from Late Cretaceous to Holocene, with the Late Paleocene sediments resting unconformably on Late Cretaceous sandstone and mudstone bedrock. Although a hiatus exists between the organic-rich (2–3%), biosilicious oozes of the middle Eocene and the sparsely fossiliferous silty clays of the Miocene, the Paleogene record recovered by ACEX is extensive, spanning from approximately 410 to 200 mbsf in depth and 56 to 44 Ma in age.

[15] Evidence for brackish conditions in the Eocene Arctic Ocean exists in sediments recently recovered by ACEX. The biosilicious assemblages of diatoms, silicoflagellates, and ebridians (as well as the organic-walled dinocysts) contained in these Eocene sediments all suggest a productive, brackish water environment [*Expedition 302 Scientists*, 2006]. Fish scales preserved with the bones sampled in the Eocene section indicate a type of smelt (G. Smith, University of Michigan Museum, personal communication, 2005), a small herbivore having a habitat consistent with the productive, brackish water environment indicated by the planktonic microfossils. Within the middle Eocene section, very rare shells of radiolarians were found in two cores. These were the only truly open marine planktonic microfossils observed in the Eocene sections. In one brief interval at the lower/middle Eocene boundary (~306 mbsf, Cores 302-M0004A-11X and 12X), abundant megaspores of the hydopterid fern *Azolla*, which is characteristic of freshwater or very low salinity environments, are present in the sediment [*Brinkhuis et al.*, 2006; *Expedition 302 Scientists*, 2006]. The *Azolla* megaspores (~50–48 Ma) are accompanied by a low branched and isoprenoid tetraether (BIT) index, indicating a minor input of organic matter by rivers, and therefore suggesting an autochthonous origin for the megaspores [*Brinkhuis et al.*, 2006]. Also notable are the low-diversity dinocyst assemblages present during the *Azolla* interval, which exhibit low numbers of marine species relative to freshwater and brackish species [*Brinkhuis et al.*, 2006].

5. Considerations in the Use of Fish Bone for Paleoenvironmental Reconstruction

[16] Reconstruction of the paleosalinity of the Norwegian-Greenland Sea, and the Arctic, is hindered by the absence of calcareous tests in the sediments, so fish bone and teeth must be utilized instead. The scarcity of fish debris in the Norwegian-Greenland Sea and the Arctic further limits $\delta^{18}O$ analysis to structurally bound carbonate within the apatite lattice, rather than the phosphate phase of the apatite itself, because the required sample size is <1 mg for analysis of structural carbonate but several milligrams for analysis of the oxygen in the phosphate phase. $\delta^{18}O$ analysis of phosphate was once preferred to analysis of structurally bound carbonate because the oxygen in the phosphate site was considered less susceptible to alteration, but the discovery of exchange between phosphate and water under microbially mediated conditions has further restricted $\delta^{18}O$ analysis of apatite for paleoecological and physiological reconstructions to the use of fossil enamel, which is usually much better preserved than bone [*Kolodny et al.*, 1996; *Zazzo et al.*, 2004]. As *Kolodny and Luz* [1991] emphasize, "in effect, every fossil fish is a pseudomorph after a fish bone" and during replacement, neither the isotopic composition of oxygen in the carbonate nor the phosphate phase of the apatite is exempt from reequilibration. Thus, although bone is rarely considered to be a reliable recorder of the life conditions of an organism, fossil bone can be useful for reconstructing paleoenvironmental conditions in the burial environment in which recrystallization occurs. The bones analyzed in this study were buried in the upper pore waters of Lomonosov Ridge, which had a water depth no greater than a few hundred meters in the Eocene [*Moore and Expedition 302 Scientists*, 2006], and should thereby provide a reasonable approximation of Arctic near-surface water salinity. *Andreasson et al.* [1996], for example, found that the carbonate of early Eocene fish apatite from the semimarine Røsnæs Clay formation and the fully marine DSDP Hole 550 gave $\delta^{18}O$ values similar to those of well-preserved foraminifera from the same samples. An added benefit of performing stable isotope analysis on the structurally bound carbonate of bone rather than phosphate is the acquisition of $\delta^{13}C$ values. In many studies $\delta^{13}C$ data are not discussed. However, *Andreasson et al.* [1996] found that the organic carbon content of the sediment seemed to have a significant

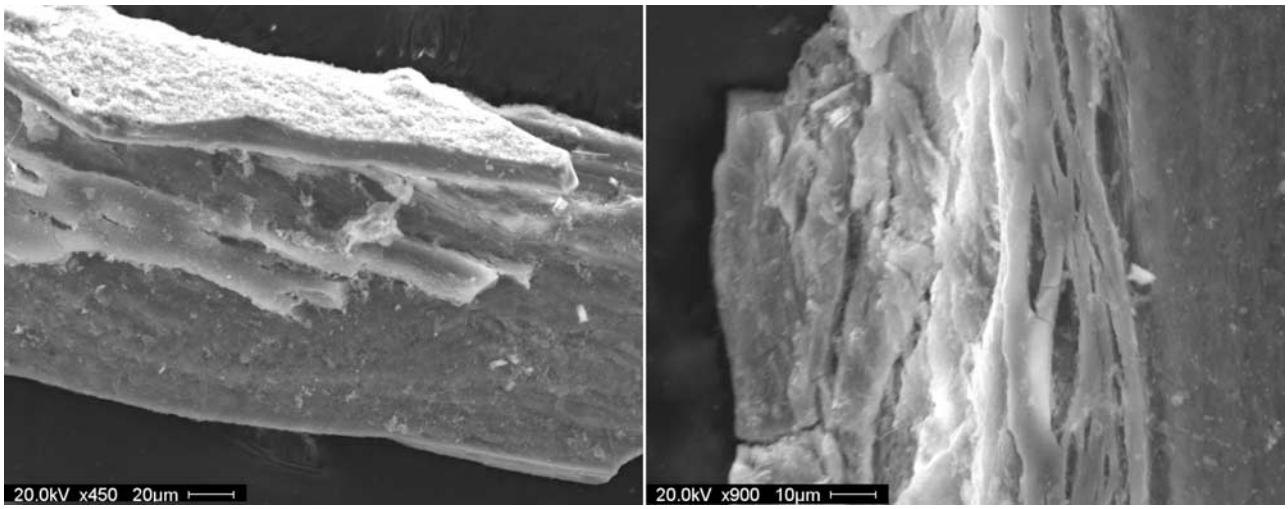

Figure 2. Secondary electron images of fish bone taken from sample 11X 2W 46–48. Authigenic flourapatite dominates the bones.

influence on the ^{13}C content of apatite, with bones found in dark organic-rich sediment tending to be more enriched in ^{12}C than those found in pale oxidized sediment.

[17] The use of fossil bone in this study involves a few considerations. First, it is possible for bones to preserve some remnant biogenic apatite, with new authigenic apatite essentially filling the intercrystalline spaces originally occupied by collagen [*Hubert et al.*, 1996; *Trueman and Tuross*, 2002]. We do not believe this to be of significance in our study, however, because the small size, thin cortical walls, and high vascular porosity of the bones make authigenic apatite growth likely to be pervasive. Examination of the bones using scanning electron microscopy with X-ray microanalysis reveals that the bones are completely overgrown by flourapatite (francolite), which is not biogenic in origin (Figure 2). If minor amounts of remnant biogenic apatite crystals do remain within the bone, we would expect the difference between the isotopic composition of the biogenic and authigenic apatite components to be relatively small because of the similarities between the life and burial environments. While some fish may have entered river mouths during their lives, the fact remains that their bones are buried on the Lomonosov Ridge in the middle of the Arctic Ocean, so it is unlikely that all of the bones analyzed belonged to fish that lived the majority of their lives in riverine environments.

[18] Second, we assume that the bones were recrystallized rapidly, ideally while near the sediment-water interface. Changes in the carbon and oxygen isotope compositions of apatite begin within days of death [*Zazzo et al.*, 2004], but bones may remain open to postmortem exchange until the pore spaces originally occupied by collagen are filled with authigenic apatite, which has been found to take up to 50 ka under some circumstances [*Kohn and Law*, 2006; *Toyoda and Tokonami*, 1990; *Trueman et al.*, 2006; *Trueman and Tuross*, 2002]. Recrystallization rates of the bones used in this study are likely to have been fast because of their small size. Additionally, we are largely concerned with variations in Arctic salinity on tectonic and long orbital timescales, so a maximum recrystallization period of 50 ka is not of great concern, and low sedimentation rates in the Arctic ($\sim$1 cm/ka), ensure that recrystallization of the bones occurred, if not at the sediment-water interface, then at least within the shallow pore waters.

6. Methods

6.1. Chemical Methods

[19] Samples were washed with distilled water over a 150 μm sieve. The coarse fraction was freeze-dried, and fish bone fragments were identified and picked from the coarse fraction under a reflecting-light microscope. Approximately 1–3 mg of bone fragments were collected from each sample, transferred to a microcentrifuge tube, and cleaned in deionized water in an ultrasonic bath for approximately 10 s, long enough to remove adhering clay without destroying the sample. Bone fragments were separated from contaminants under a microscope, ground into a powder with a mortar and pestle, returned to a preweighed microcentrifuge tube, and dried in the oven at 40°C.

[20] Fish bone samples were then chemically treated using the method recommended by *Koch et al.* [1997]. Bone powders were soaked in 2% NaOCl for 24 h to oxidize organic matter, rinsed five times with deionized water, and centrifuged between each rinse. The treatment was repeated using 1 M acetic acid-calcium acetate buffer to remove diagenetic carbonates. Samples were then roasted under vacuum at 200°C for 1 h.

[21] The carbon and oxygen isotope composition of the fish bone carbonate was analyzed in the University of Michigan Stable Isotope Laboratory. Samples were reacted at 75°C with phosphoric acid in a Kiel automatic carbonate preparation device linked to a Finnigan MAT 251 mass spectrometer. Stable isotope data are reported in standard δ notation relative to the Vienna Peedee belemnite (VPDB) standard. Because the structural carbonate content of bone is $\sim$4% [*Koch et al.*, 1997], only samples weighing more than

Table 1. Chemical Treatment Test Performed on Sample M0002A-55X-CC

	Mass, mg	δ^{13}C (VPDB)	δ^{18}O (VPDB)
Untreated 1	1.2	−13.85	−4.19
Untreated 2	1.2	−13.71	−3.73
Average untreated		−13.78	−3.96
Treated 1	1.7	−13.97	−3.55
Treated 2	1.5	−14.02	−3.37
Average treated		−14.00	−3.46
Treated-untreated		−0.2	+0.5

0.8 mg following chemical treatment consistently generated enough CO_2 for analysis. Analytical precision, which was monitored through the regular analysis of the standard reference carbonate NBS-19, was better than ±0.1‰ (1σ) for both δ^{18}O and δ^{13}C. The isotopic variability of a single powder following treatment was found to be ±0.4‰ for δ^{18}O and ±0.2‰ for δ^{13}C (1σ, N = 11).

[22] In subjecting bone samples to a chemical treatment procedure, uniformity in the concentration, amount of solutions used, and the duration of each treatment step is crucial to achieving results with a consistent isotopic offset [*Koch et al.*, 1997]. *Koch et al.* [1997] found that treated bone samples from land mammals consistently show more positive δ^{18}O values and more negative δ^{13}C values than untreated samples. For example, chemical treatment of ACEX sample 2A-55X-CC with 2% NaOCl and 1M acetic acid-calcium acetate buffer produced a mean shift of approximately +0.5‰ for δ^{18}O and −0.2‰ for δ^{13}C as compared with untreated samples (Table 1). The magnitude of the offset, however, can increase when more concentrated acids or longer treatment times are used, possibly the result of progressive dissolution of weakly bonded carbonate within the structural lattice [*Koch et al.*, 1997]. Thus, to minimize errors associated with chemical treatment, samples used in this study were treated simultaneously in order to ensure identical chemical conditions, with the exception of the samples older than 50.4 Ma and the Miocene sample 44X-CC, which were treated at a later date.

6.2. Estimation of Salinity

[23] When reasonable independent temperature estimates exist, salinity can be estimated by first calculating the δ^{18}O value of the water mass ($\delta^{18}O_w$) using the paleotemperature equation of *Friedman and O'Neil* [1977],

$$10^3 \ln \alpha_{CaCO3\text{-}water} = 2.78 \times 10^6/T^2 - 2.89,$$
$$\text{where } \alpha_{CaCO3\text{-}water} = \left(\delta^{18}O_{CaCO3} + 10^3\right)/\left(\delta^{18}O_w + 10^3\right)$$

and then by applying the $\delta^{18}O_w$-salinity relation.

[24] Salinity and $\delta^{18}O_w$ are linearly related, with a slope $\Delta\delta^{18}O_w/\Delta S$ that varies regionally because of Rayleigh distillation of precipitation and a zero-salinity intercept that reflects the δ^{18}O value of the local precipitation and runoff. In modern open ocean surface waters, $\Delta\delta^{18}O_w/\Delta S$ ranges between 0.1 in the tropics and 0.6 in the high latitudes [*Craig and Gordon*, 1965], although variations have been noted in marginal seas. In regions with sea ice, a high slope and a "fictitious" zero-salinity intercept with a δ^{18}O value much lower than the δ^{18}O of precipitation ($\delta^{18}O_p$) is possible because of the rejection of salt without any significant fractionation of δ^{18}O [*Zahn and Mix*, 1991]. Several equations relating $\delta^{18}O_w$ and salinity in the North Atlantic and

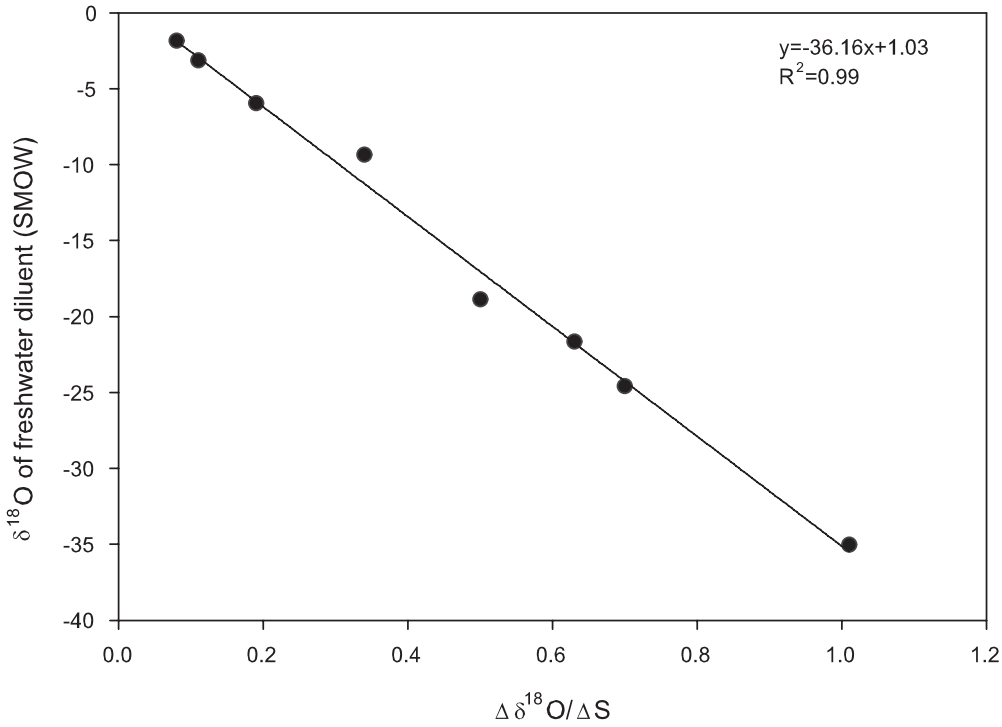

Figure 3. Results of a linear regression performed on the zero-salinity intercepts and slopes of the $\delta^{18}O_w$-salinity equations listed in Table 2 for the North Atlantic and Arctic.

Table 2. $\delta^{18}O_w$–Salinity Relation for Sites in the Arctic and North Atlantic Obtained From Surface Water Measurements Across Diverse Modern Salinity Gradients

Study Region	Equation	Source
East Greenland	$\delta^{18}O_w$ – 1.01S–35.02	*Fairbanks et al.* [1992]
Central Arctic	$\delta^{18}O_w$ – 0.7S–24.6	*Vetshteyn et al.* [1974]
Slope water	$\delta^{18}O_w$ – 0.63S–21.67	*Fairbanks et al.* [1992]
Laptev Sea	$\delta^{18}O_w$ – 0.50S–18.86	*Mueller–Lupp et al.* [2003]
German Bight, North Sea	$\delta^{18}O_w$ – 0.34S–9.36	*Scheurle and Hebbeln* [2003]
Western equatorial Atlantic	$\delta^{18}O_w$ – 0.19S–5.97	*Fairbanks et al.* [1992]
Sargasso Sea and Gulf Stream	$\delta^{18}O_w$ – 0.11S–3.15	*Fairbanks et al.* [1992]
Eastern equatorial Atlantic	$\delta^{18}O_w$ – 0.08S–1.86	*Fairbanks et al.* [1992]

Arctic are shown in Table 2. The slope $\Delta\delta^{18}O_w/\Delta S$ and the zero-salinity intercept of the $\delta^{18}O_w$-salinity relation are ideally linearly related, and a linear regression performed on these parameters from Table 2 gives the equation y = −36.16 * ($\Delta\delta^{18}O_w/\Delta S$) +1.03, where y is the $\delta^{18}O$ value of the freshwater diluent (Figure 3). Thus, if reasonable estimates exist for the $\delta^{18}O$ value of the regional runoff, then it is possible to calculate a corresponding value for the slope $\Delta\delta^{18}O_w/\Delta S$. Because terrestrial paleoprecipitation proxies have provided estimates for the value of $\delta^{18}O_p$ in the Eocene Arctic [*Bice et al.*, 1996; *Jahren and Sternberg*, 2002; *Tripati et al.*, 2001], we assume in this study that $\delta^{18}O_p$ provides a reasonable approximation of the $\delta^{18}O$ value of the regional runoff in the Arctic.

7. Results and Discussion

7.1. Oxygen Isotopes

[25] Stable isotope results were acquired from approximately 30 samples from Holes M0002A and M0004A with ages of ∼55 to ∼45 Ma (Figures 4a and 4b and Table 3). A single sample of middle Miocene age (∼18 Ma) was also analyzed. The $\delta^{18}O_{CO3}{}^{2-}$ values of the Eocene samples range from −6.84‰ to −3.03‰, with a mean value of −4.89‰. The lowest $\delta^{18}O$ value occurs at ∼48.7 Ma ($\delta^{18}O$ = −6.84‰ for sample M0004A-11X-3W 46–48), and exceptionally low values were also obtained at ∼55 Ma ($\delta^{18}O$ = −6.45‰ and −6.20‰ for samples M0004A-31X-CC and 30X-CC, respectively) and ∼47.6 Ma ($\delta^{18}O$ = −6.83‰ and −6.08‰ for samples M0004A-6X-1W 82–84 and 6X-2W 82–84, respectively). Overall, the middle Miocene sample (M0002A-44X-CC) gave the highest $\delta^{18}O$ value ($\delta^{18}O$ = 2.77‰), but of the Eocene samples, the highest value occurs at ∼46.3 Ma in sample M0002A-56X-CC ($\delta^{18}O$ = −3.03).

[26] The low $\delta^{18}O$ values recorded at ∼55 Ma in samples M0004A-31X-CC and 30X-CC likely reflect a warming and freshening of the Arctic during the PETM. Samples 31X-CC and 30X-CC are characterized by the presence of the diagnostic dinocyst species *Apectodinium augustum*, which is typical of tropical to subtropical environments but which expanded its distribution during the warm climates of the PETM [*Moran et al.*, 2006].

[27] In the middle Eocene, the negative $\delta^{18}O$ excursion at ∼48.7 Ma in sample M0004A-11X-3W 46–48 corresponds with the *Azolla* event. The excursion therefore reflects a freshening of the surface waters contemporaneous with the brief expansion of the freshwater fern into the Arctic Ocean. The negative excursion at ∼47.6 Ma in sample M0004A-6X-1W 82–84 probably indicates a third freshwater event. *Stickley et al.* [2008] observe the first abundant occurrence of *Anulus arcticus*, a diatom thought to be tolerant of low salinities, at ∼47.6 Ma, adding support for a significant change in surface water conditions during this period.

[28] The positive $\delta^{18}O$ excursion at ∼46.3 Ma found in samples M0002A-56X-CC and 55X-CC may represent a brief increase in Arctic salinity. *Stickley et al.* [2008] interpret a peak in diatom abundance during this interval as possible evidence that conditions were less brackish. Isolated dropstones were found in Hole M0002A as deep as Section 55X-4 [*Expedition 302 Scientists*, 2006], so it is also possible that the positive $\delta^{18}O$ excursion may represent an interval of significant cooling near the time of the first appearance of icebergs in the Arctic [*Moran et al.*, 2006; *St. John and Willard*, 2006]. The positive excursion at ∼46.3 Ma could therefore reflect a combination of cooler conditions and diminished runoff, and may have been a manifestation of the larger cooling trend from the early middle Eocene through the early Oligocene [*Zachos et al.*, 2001].

[29] By ∼18 Ma, a significant shift toward normal marine salinities and cooler temperatures had taken place in the Arctic, as indicated by the very high $\delta^{18}O$ value of 2.77‰ obtained from Miocene sample M0002A-44X-CC. This result is in sharp contrast to the mean $\delta^{18}O$ value of −4.89‰ obtained from the Eocene bone samples. Sample 44X-CC occurs slightly above the ∼30 Ma hiatus that separates the middle Eocene and Miocene sediments in Hole M0002A. Part of the shift toward a higher $\delta^{18}O$ value could be explained by the subsidence of the ridge to a depth of ∼1000 m by the mid-Miocene, as proposed by *Moore and Expedition 302 Scientists* [2006], and could therefore reflect the burial and alteration of the fish remains under higher-salinity conditions at depth in the water column. Overall, however, the higher $\delta^{18}O$ value of the Miocene sample supports an erosional cause for the hiatus associated with the introduction of North Atlantic waters to the Arctic Ocean [*Jakobsson et al.*, 2007].

7.2. Carbon Isotopes

[30] The $\delta^{13}C$ values of the Eocene Arctic samples range between −16.98‰ and −8.90‰, with a mean value of −12.18‰, and the middle Miocene sample M0002A-44X gave a $\delta^{13}C$ value of −5.25‰. The lowest Eocene $\delta^{13}C$ values of −16.98‰ and −16.96‰ were recorded in the PETM samples M0004A-31X-CC and 30X-CC, respectively, and the highest value of −8.90‰ was from sample 11X-3W 46–48 cm, which corresponds to the *Azolla*

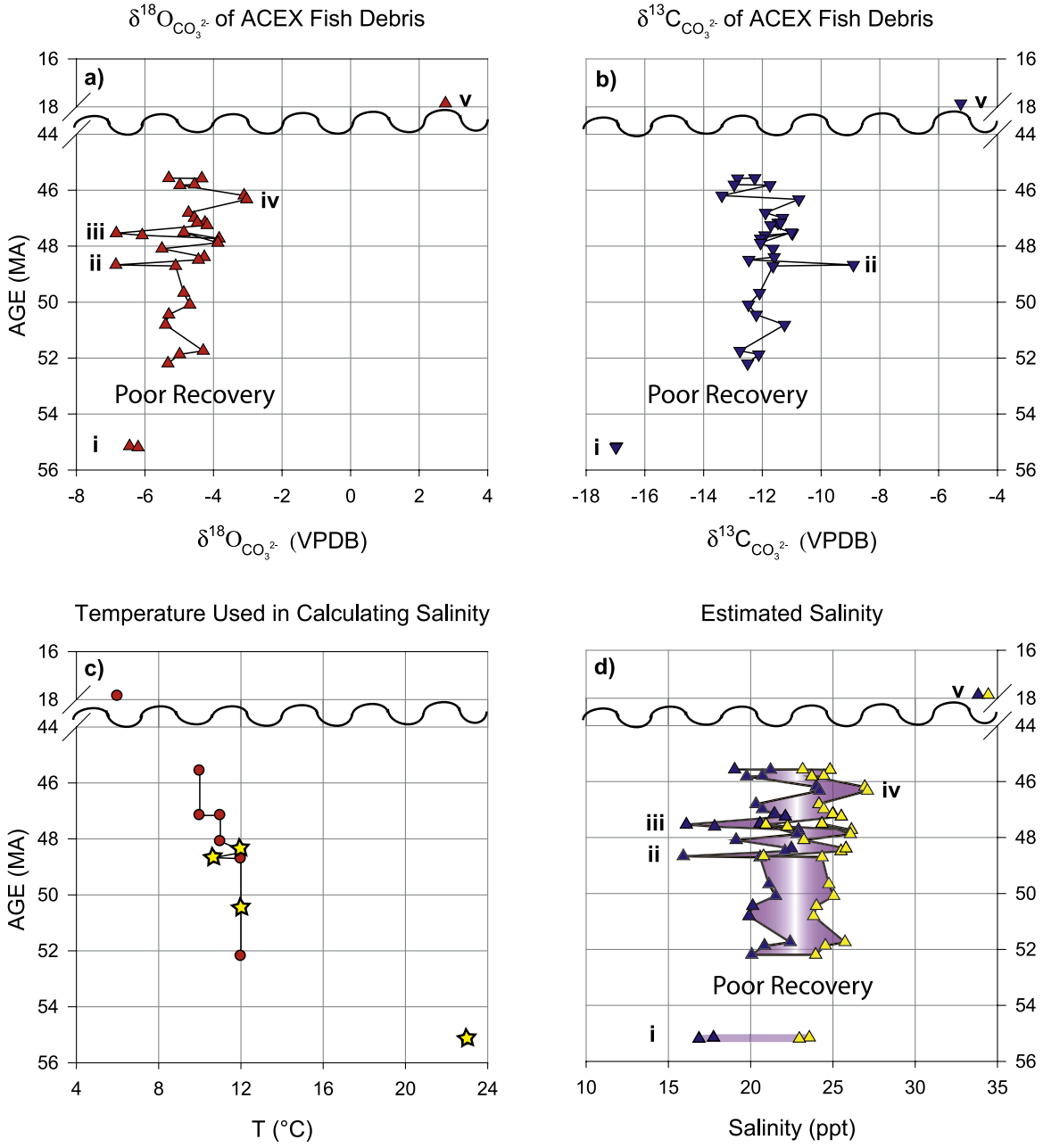

Figure 4. (a) Oxygen and (b) carbon isotopic composition of fish debris from IODP Expedition 302 Holes M0002A and M0004A. Ages are based on *Backman et al.* [2008], and the wavy line indicates a hiatus. Features of interest include negative $\delta^{18}O$ excursions at 55 Ma (Paleocene-Eocene thermal maximum) (labeled i), 48.7 Ma (*Azolla* event) (labeled ii), and 47.6 Ma (labeled iii), as well as positive $\delta^{18}O$ excursions at 46.3 Ma (labeled iv) and 17.9 Ma (labeled v). Also of interest are a negative $\delta^{13}C$ excursion at time i and relatively positive $\delta^{13}C$ values at times ii and v. (c) Temperatures used in calculating Arctic salinity. Stars indicate independent temperature estimates from ACEX material made by *Sluijs et al.* [2006] and *Brinkhuis et al.* [2006]. For the other intervals, it was necessary to approximate temperatures based on the results of other Eocene paleotemperature studies, as described in the text. (d) Calculated salinity range based on $\delta^{18}O$ data in Figure 4a and temperatures shown in Figure 4c. Minimum salinity was calculated by assuming $\delta^{18}O_p = -15‰$, and maximum salinity was calculated using $\delta^{18}O_p = -20‰$, except at the PETM where a $\delta^{18}O_p$ range of -10 to $-15‰$ was used.

Table 3. Stable Isotope Data Generated From the Analysis of Fish Bones in ACEX Holes 302 M0002A and M0004A and the Calculated Salinity Range for Each Sample

	Stable Isotope Results								Calculated Salinity	
									Salinity	
Hole, Core, Section, and Interval, cm	Weight, mg	mcd, m	Age, Ma	δ^{13}C (VPDB)	δ^{18}O (VPDB)	Average δ^{13}C (VPDB)	Average δ^{18}O (VPDB)	δ^{18}O (SMOW)	T[a] (°C)	Min	Max
2A-44X-CC	1.2	195.91	17.86	−5.25	2.77[b]	−5.25	2.77	0.42	6	35.09	35.40
2A-52X-1 140–150	1.4	226.41	45.57	−12.26	−5.30	−12.26	−5.30	−6.64	10	19.03	23.16
2A-52X-CC	3.4	226.73	45.58	−12.90	−4.32	−12.84	−4.34	−5.68	10	21.21	24.83
	2.2			−12.78	−4.36						
2A-53X-CC	2.1	231.96	45.80	−12.96	−4.56	−12.96	−4.56	−5.89	10	20.72	24.46
2A-54X-CC-bott	1.0	232.5	45.82	−11.75	−4.98	−11.75	−4.98	−6.31	10	19.76	23.72
2A-55X-bott-CC	1.6	241.42	46.19	−13.26	−3.16	−13.38	−3.105	−4.46	10	23.98	26.94
	1.7			−13.49	−3.05						
2A-56X-CC-bott	2.4	244.8	46.33	−10.63	−3.10	−10.76	−3.03	−4.37	10	24.19	27.10
	1.7			−10.88	−2.96						
2A-58X-CC-bott	1.7	256.61	46.81	−11.96	−4.69	−11.90	−4.73	−6.07	10	20.33	24.15
	1.7			−11.83	−4.76						
2A-59X-CC 0–2	1.0	260.81	46.99	−11.31	−4.56	−11.31	−4.56	−5.89	10	20.71	24.45
2A-60X-CC	1.3	265.07	47.16	−11.47	−4.25	−11.47	−4.25	−5.58	10	21.43	24.99
4A-4X-1 top (0–3)	2.9	265.015	47.16	−11.38	−4.47	−11.38	−4.47	−5.56	11	21.47	25.02
2A-61X-CC 4–6	2.8	267.22	47.25	−11.76	−4.00	−11.71	−4.19	−5.28	11	22.12	25.52
	2.5			−11.66	−4.37						
2A-62X-CC 9–11	2.2	273.51	47.51	−11.01	−4.86	−11.01	−4.86	−5.96	11	20.57	24.34
4A-6X-1W 82–84	1.0	274.33	47.54	−10.97	−6.83	−10.97	−6.83	−7.93	11	16.09	20.93
4A-6X-2W 82–84	1.4	275.83	47.61	−11.91	−6.08	−11.91	−6.08	−7.17	11	17.81	22.24
4A 6X-CC bott	1.4	278.78	47.73	−12.06	−3.83	−12.06	−3.83	−4.93	11	22.92	26.13
4A-8X-CC bott	1.8	282.58	47.88	−12.20	−3.97	−12.06	−3.87	−4.96	11	22.83	26.06
	1.3			−11.92	−3.76						
4A-9X-CC bott	0.6	287.66	48.09	−11.64	−5.50	−11.64	−5.50	−6.60	11	19.12	23.23
4A-10X-2 147–150 cm	1.8	294.84	48.39	−11.59	−4.27	−11.59	−4.27	−5.12	12	22.48	25.79
4A-10X-CC bott	2.3	297.19	48.49	−12.46	−4.44	−12.46	−4.44	−5.29	12	22.09	25.50
4A-11X-3W 46–48	1.4	300.78	48.67	−8.90	−6.84	−8.90	−6.84	−8.01	10.7	15.91	20.79
4A-12X-CC bott	1.5	301.37	48.71	−11.64	−5.10	−11.64	−5.10	−5.95	12	20.58	24.35
4A-15X-CC bott	2.7	313.61	49.67	−12.10	−4.87	−12.10	−4.87	−5.72	12	21.11	24.75
4A-18X-CC bott	2.7	318.96	50.09	−12.47	−4.69	−12.47	−4.69	−5.54	12	21.51	25.06
4A-19X-CC top[c]	1.0	323.54	50.45	−12.21	−5.30	−12.21	−5.30	−6.15	12	20.13	24.00
4A-20X-CC top[c]	1.5	328.07	50.81	−11.25	−5.40	−11.25	−5.40	−6.25	12	19.90	23.83
302-M4A-22X-CC bott[c]	0.9	339.98	51.74	−12.76	−4.30	−12.76	−4.30	−5.15	12	22.41	25.74
302-M4A-23X-1 top[c]	1.0	341.6	51.87	−12.12	−4.98	−12.12	−4.98	−5.84	12	20.84	24.55
302-M4A-23X-CC bott[c]	1.8	345.67	52.19	−12.50	−5.33	−12.50	−5.33	−6.18	12	20.07	23.96
302-M4A-30X-CC bott[c]	1.4	384.54	55.15	−16.96	−6.45	−16.96	−6.45	−4.64	22.7	17.74	23.57
302-M4A-31X-CC bott[c]	1.5	385.25	55.19	−16.98	−6.20	−16.98	−6.20	−4.90	22.6	16.86	22.97

[a]Temperatures for samples 4A-30X and 31X are from *Sluijs et al.* [2006], 4A-11X is from *Brinkhuis et al.* [2006], and 4A-19X is from A. Sluijs (personal communication, 2006). Temperatures for the other samples are approximated.

[b]The δ^{18}O value corrected by +1.5‰ because replicate samples treated alongside sample 2A-44X-CC in a later batch were found to be consistently more negative than previous analyses by this amount.

[c]Separate treatment batch from other samples.

event. With high TOC contents (1.5 to >3 wt %) in the Eocene Arctic sediments as compared to the Miocene and younger sediments (<0.4 wt %) [*Expedition 302 Scientists*, 2005], it appears that bones buried in sediment with a higher TOC content tend to exhibit lower δ^{13}C values than those buried in a more oxidizing environment [*Andreasson et al.*, 1996].

[31] In the case of the PETM samples, the addition of 2000–4000 Gt of light carbon to the atmosphere at the PETM resulted in an ∼−6‰ shift in the δ^{13}C value of the terrestrial organic matter and TOC buried in the ACEX sediments [*Pagani et al.*, 2006], so the exposure of the fish bones to the ^{12}C-rich organic sediment during diagenesis can therefore explain the light carbon isotopic composition recorded in samples 31X-CC and 30X-CC. During the *Azolla* event at ∼49 Ma, however, the TOC content of the sediment reaches a maximum of 4.2 wt% [*Expedition 302 Scientists*, 2005], while the carbon isotope composition of the bones is the highest of all of the Eocene samples. *Azolla* represents a symbiotic relationship in which cyanobacteria perform nitrogen fixation for a fern. Thus, during the *Azolla* event, abundant nitrogen provided by the cyanobacteria and a plentiful supply of phosphorus from increased river runoff would have resulted in an increase in primary production in the Arctic. In studying mid-Pleistocene sapropels from the Mediterranean, *Meyers and Bernasconi* [2005] found that during periods of wet climate conditions and high cyanobacterial primary production, the organic δ^{13}C values in the sediments increased by ∼3–5‰ above background levels because of the depletion of ^{12}C in the surface waters. The positive δ^{13}C excursion observed in sample M0004A-11X-3W 46–48 cm during the *Azolla* event may therefore be attributable to the burial of the fish bones with ^{13}C-enriched organic matter during a period of extreme primary productivity.

7.3. Salinity Reconstruction for the Arctic Ocean

[32] In order to calculate the salinity of the Arctic Ocean during the early and middle Eocene, reasonable constraints are needed for temperature and the $\delta^{18}O$ value of local precipitation and runoff. TEX_{86} estimates have been made from ACEX Hole M0004A at the PETM, the *Azolla* event, and ~50 Ma (sample 4A-19X-CC), and thus provide good constraints for early Eocene conditions. Using TEX_{86}', *Sluijs et al.* [2006] found that sea surface temperatures (SSTs) in the Arctic exhibited extreme warmth during the PETM, rising from 18°C in the Late Paleocene to over 23°C during the PETM (top of Core 32X to within Core 29X), and subsequently decreasing to ~17°C following the event. By ~50 Ma, SSTs had cooled to 12°C (A. Sluijs, personal communication, 2006), and TEX_{86} results show that at the *Azolla* event, temperatures had decreased further to 10°C but recovered to 12°–14°C following the event [*Brinkhuis et al.*, 2006].

[33] For the early middle Eocene, where TEX_{86} estimates were not available from the ACEX sites, it was necessary to approximate temperatures from the results of regional reconstructions. In general, SSTs were warmer at the beginning of the ~10 Ma spanned by the $\delta^{18}O_{CO3}{}^{2-}$ record than at the end. Maximum high-latitude Southern Ocean SSTs of 10°–12°C were recorded by foraminifera during the late Paleocene and early middle Eocene, as compared to 15°C during the early Eocene and 6°C by the late Eocene [*Zachos et al.*, 1994]. Global deepwater temperatures of ~12°C were obtained by *Lear et al.* [2000] at ~47 Ma from Mg/Ca data, declining to ~10°C by 45 Ma. Arctic terrestrial proxies give comparable results. Analysis of secondary calcite in fossil *Metasequoia* wood from Axel Heiberg Island yielded a terrestrial mean annual temperature of 13.2 ± 2.0°C for the middle Eocene [*Jahren and Sternberg*, 2003], while a multiple regression model of foliar physiognomy and floristic composition on Axel Heiberg and Ellesmere Islands estimated a mean annual temperature of 8.2°–9.3°C during the middle Eocene, with a mean annual temperature range spanning 14°C [*Greenwood and Wing*, 1995]. Thus, taking into consideration these estimates, we choose to use a temperature of 12°C in our salinity reconstruction for the early middle Eocene and decrease the value to 10°C by ~45 Ma, as shown in Table 3 and Figure 4c.

[34] As for local precipitation and runoff, the $\delta^{18}O$ value of the modern mean freshwater diluent in the North Atlantic is −20.6‰ [*Craig and Gordon*, 1965], and Arctic runoff has a very similar average value [*Bauch et al.*, 1995]. Studies of bivalves by *Bice et al.* [1996] and *Tripati et al.* [2001] estimated $\delta^{18}O$ values for the late Paleocene freshwater diluent of ~23.5‰ on the North Slope of Alaska and ~−20 to −22‰ on Ellesmere Island, respectively. Studies of fossil cellulose from Axel Heiberg Island by *Jahren and Sternberg* [2002] yielded a slightly higher $\delta^{18}O$ value of −15.1‰ for meteoric water during the mid to late Eocene. Overall, however, a reduction in the global temperature gradient and higher condensation temperatures in the Arctic during the Paleogene do not appear to have led to significantly higher $\delta^{18}O$ values in high-latitude precipitation. Instead, Rayleigh distillation during meridional vapor transport seems to have had a dominant influence over the $\delta^{18}O$ value of Arctic precipitation during the Paleogene [*Jahren and Sternberg*, 2002; *Tripati et al.*, 2001]. Thus, because the $\delta^{18}O$ value of Eocene precipitation was not dramatically different from that of the present day, in reconstructing the salinity of the Eocene Arctic Ocean we choose to use $\delta^{18}O_p$ values between −15 and −20‰ and thereby calculate corresponding $\Delta\delta^{18}O_w/\Delta S$ slopes of 0.44 to 0.58. Thus, a minimum salinity was calculated for each sample interval by assuming $\delta^{18}O_p = -15‰$, and a maximum salinity was calculated using $\delta^{18}O_p = -20‰$, except at the PETM, where higher $\delta^{18}O_p$ values of −10 to −15‰ were used in conjunction with smaller slopes of 0.30 and 0.44, respectively, based on the results of *Pagani et al.* [2006].

[35] Thus, using a mean temperature of 12°C, a $\delta^{18}O$ value of precipitation and runoff between −15‰ and −20‰, corresponding $\Delta\delta^{18}O_w/\Delta S$ slopes of 0.44 and 0.58, respectively, and a mean $\delta^{18}O_{CO3}{}^{2-}$ value of −4.89‰, we calculated an average salinity in the Arctic of ~21 to 25‰ during the early and middle Eocene. By comparison, for middle Miocene sample M0002A-44X-CC, using the same parameters for the $\delta^{18}O$ of precipitation and runoff as for the Eocene samples but a lower mean temperature of 6°C estimated from *Lear et al.* [2000], we calculated a salinity of the Arctic Ocean of ~35‰, which is slightly high for a modern Arctic surface water salinity but essentially denotes full marine conditions in the Arctic by the early Miocene. A reconstruction demonstrating the large-scale variation of Arctic salinity is shown in Figure 4d, salinity estimates are given in Table 3, and results for key intervals are compared in Table 4.

[36] Because many of our salinity estimates depend on assumed temperatures, we demonstrate in Table 4 the sensitivity of our salinity calculations to temperature over a range of ±3°C. As can be seen from this, our salinity estimates are not highly sensitive to temperature. Adding an error of ±3°C to our estimated temperatures expands our salinity estimates ~1.5–2‰ on either side of the calculated range, and thus our average Eocene salinity estimate changes from ~21–25‰ to ~19.4–26‰.

[37] Additionally, the salinity estimates obtained in this study are not expected to reflect the full extent of freshening in the Arctic surface waters. *Onodera et al.* [2007] suggest that the co-occurrence of fresh and brackish water microfossils in the ACEX sediments can be explained by the existence of a strong halocline that divided the upper water column into a fresh surface layer and a brackish habitat below. Thus, fish bones buried and altered on the Lomonosov Ridge at a depth of a few hundred meters would probably record the salinity of a lower brackish water layer rather than that of the uppermost freshwater lens.

7.4. Paleocene-Eocene Thermal Maximum

[38] Using the TEX_{86}' temperature estimate of 23°C made from ACEX material by *Sluijs et al.* [2006] for the PETM and the $\delta^{18}O_{CO3}{}^{2-}$ values of −6.45‰ and −6.20‰ obtained from samples M0004A-31X-CC and 30X-CC, respectively, we estimate salinity in the Arctic Ocean at ~17–24‰ during the PETM. Because the SST estimates were made using TEX_{86}', the results may be skewed toward the summer season when phytoplankton productivity was at a maximum,

Table 4. Estimates of Arctic Salinity Based on Different Assumptions of $\Delta\delta^{18}O_w/\Delta S$, $\delta^{18}O$ of Precipitation ($\delta^{18}O_p$), and Temperature for the PETM, the *Azolla* Event, 47.6 Ma (a Possible Low-Salinity Event), 46.3 Ma (a Possible High-Salinity Event), Average Eocene Conditions, and Miocene Sample 44X-CC

Sample	Age, Ma	$\delta^{18}O$ CO_3^{2-} (VPDB)	$\delta^{18}O_w$ (SMOW)	T, °C	$\delta^{18}O_p$ (SMOW)	Assumed $\Delta\delta^{18}O_w/\Delta S$	Salinity, ‰	T Sensitivity: Salinity, ‰ (T − 3°C)	T Sensitivity: Salinity, ‰ (T + 3°C)
4A-30X-CC bott (PETM)	55.15	−6.45	−4.39	22.7[a]	−10[b]	0.30	17.74	15.59	19.83
					−15	0.44	23.57	22.09	25.01
4A-31X-CC bott (PETM)	55.19	−6.20	−4.64	22.6[a]	−10[b]	0.30	16.86	14.70	18.95
					−15	0.44	22.97	21.48	24.40
4A-11X-3W 46–48 (*Azolla* Event)	48.67	−6.84	−8.21	10.7[c]	−15	0.44	15.91	14.24	17.53
					−20	0.58	20.79	19.51	22.02
4A-6X-1W 82–84	47.54	−6.83	−7.93	11	−15	0.44	16.09	14.43	17.71
					−20	0.58	20.93	19.66	22.16
2A-56X-CC-bott	46.33	−3.03	−4.37	10	−15	0.44	24.19	22.50	25.83
					−20	0.58	27.10	25.81	28.34
Eocene Average	55–45	−4.89	−5.54	12	−15	0.44	21.06	19.41	22.66
					−20	0.58	24.71	23.45	25.93
Miocene	17.86	2.77	0.42	6	−15	0.44	35.09	33.31	36.80
					−20	0.58	34.40	34.05	36.71

[a] *Sluijs et al.* [2006].
[b] *Pagani et al.* [2006].
[c] *Brinkhuis et al.* [2006].

and therefore salinities could have actually been slightly lower than these estimates by a few parts per thousand. The results show that salinity at the PETM might have been significantly lower than the Eocene average, but the very negative $\delta^{18}O_{CO3}{}^{2-}$ values obtained from the interval may largely be the result of extreme sea surface temperatures.

[39] *Pagani et al.* [2006] report a significant decrease in the extent of Rayleigh distillation of precipitation in the Arctic during the PETM, as indicated by the hydrogen isotope compositions of the high molecular weight *n*-alkane *n*-C_{29}. During the peak warmth of the early phase of the PETM, *Pagani et al.* [2006] estimate that spring precipitation in the Arctic had a δD value of ∼−30 to −55‰, which corresponds through the meteoric water line to a $\delta^{18}O$ value in the range of −5 to −8‰. Such high δD and $\delta^{18}O$ values are usually associated with precipitation in the subtropics and may indicate an increase in the delivery of water vapor to the Arctic as a result of decreased rainout of subtropical water in the midlatitudes under reduced meridional and vertical temperature gradients [*Pagani et al.*, 2006]. However, as the PETM progressed, *Pagani et al.* [2006] obtained lower δD values of ∼−70 to −115‰, which correspond to $\delta^{18}O$ values in the range ∼−10 to −15‰. Thus, because the samples examined in this study (M0004A-31X-CC and 30X-CC) are from the latter portion of the PETM, the salinity estimates obtained may not reflect the full extent of surface water freshening possible in the region during conditions of peak warmth.

7.5. The *Azolla* Event and Middle Eocene Salinity Variations

[40] We calculated an Arctic salinity of ∼16–21‰ during the *Azolla* event at ∼48.7 Ma using the temperature estimate of 10.7°C made by *Brinkhuis et al.* [2006] and a $\delta^{18}O_{CO3}{}^{2-}$ value of −6.84‰ from sample M0004A-11X-3W 46–48. The *Azolla* event appears in our salinity reconstruction as one the lowest-salinity periods in the Eocene, and unlike the PETM, during which freshening of the surface waters was probably associated with an increase in regional precipitation, the *Azolla* event was likely the result of the increased isolation of the Arctic during a sea level lowstand. The timing of the *Azolla* event is consistent with a sea level lowering reported by *Miller et al.* [2005b] at ∼49 Ma during chron C21r, and a slight decline in Arctic SSTs as reported by *Brinkhuis et al.* [2006] suggests decreased communication with the Atlantic during the event. Similarly, a sudden temperature increase of 3°–4°C following the event probably signals the renewed influx of salt and heat to the Arctic after sea level had been restored [*Brinkhuis et al.*, 2006]. *Radionova and Khokhlova* [2000] report that the Arctic connection to the world ocean through the Turgay Strait ceased to exist at ∼49 Ma, and considering that a substantial percentage of the surface area of the Arctic Ocean is continental shelf, the migration of river mouths closer to the center of the Arctic Ocean during a lowstand could also have contributed to decreased salinity on the Lomonosov Ridge.

[41] Other significant middle Eocene salinity variations occur in our reconstruction at ∼47.6 Ma, where we calculated a salinity low of ∼16–21‰ using a temperature of 11°C and a $\delta^{18}O_{CO3}{}^{2-}$ value of −6.83‰ from sample M0004A-6X-1W 82–84, and at ∼46.3 Ma, where we calculated a salinity high of ∼24–27‰ using a temperature of 10°C and a $\delta^{18}O_{CO3}{}^{2-}$ value of −3.03‰ from sample M0002A-56X-CC. Because TEX_{86} estimates were not available for these samples, errors in our temperature estimates are potentially significant. Thus, the low-salinity event in our reconstruction at ∼47.6 Ma could correlate

Table 5. Comparison Between Stable Isotope Values Obtained From Early Eocene Untreated Fish Bone and Teeth From ODP Hole 913B in the Norwegian-Greenland Sea and Full Marine DSDP Hole 550 in the Northeastern Atlantic by *Andreasson et al.* [1996] and This Study

	$\delta^{18}O$	$\delta^{13}C$
Andreasson et al. [1996]		
151-913B-		
46R-CC	−6.73	−9.26
47R-1, 108–110	−7.78	−9.25
48R-CC	−8.23	−10.11
49R-3 118–121	−7.28	−8.00
50R-4 94–97	−6.70	−4.56
80-550-		
24-	−1.35	−0.09
24-1 135–138	−0.17	−0.14
This Study		
151-913B-		
Mixture of 48 2W 23.5–25, 46 3 21–22.5, 50 4W 81.5–83, 49 2W 54.5–66.5	−8.44	−8.34
80-550-		
24R-3 52–60	0.17	0.17

with the early middle Eocene sea level lowstand of *Miller et al.* [2005b] at ~48 Ma during chron 21n, and thus closely resemble the *Azolla* event in origin. However, as shown in Table 4, a temperature increase of ~3°C at 47.6 Ma could partially account for this negative $\delta^{18}O$ excursion, although no evidence for such a warm interval currently exists. Similarly, the high-salinity event ~46.3 Ma in our reconstruction could alternatively be explained by a decrease in temperature of ~3°C, as shown in Table 4, which is supported by the first appearance of isolated dropstones on the Lomonosov Ridge at ~46 Ma [*Moran et al.*, 2006; *St. John and Willard*, 2006].

7.6. Comparison to the Norwegian-Greenland Sea

[42] Overall, the $\delta^{18}O_{CO3}{}^{2-}$ values obtained in this study for the Eocene Arctic Ocean, which range from −6.84‰ to −2.96‰, are higher than those obtained by *Andreasson et al.* [1996] from ODP Hole 913B for the Eocene Norwegian-Greenland Sea (−6.70‰ to −8.23‰). Analysis of untreated Eocene fish debris from Hole 913B and fully marine northeastern Atlantic ODP Hole 550 in this study yielded stable isotope values very similar to those obtained by *Andreasson et al.* [1996] (Table 5). Thus, differences in interlaboratory methods can be ruled out, and although the Arctic Ocean samples were chemically treated prior to analysis while the Hole 913B samples were not, the increases in $\delta^{18}O$ expected from chemical treatment are too small to account for the differences in $\delta^{18}O$ observed between the two localities. The mixing of bones and teeth in the Hole 913B samples could have shifted the $\delta^{18}O$ results toward lower values because teeth are less susceptible to alteration than bone and might therefore better preserve the surface water signal, but *Andreasson et al.* [1996] found no significant difference between samples composed only of teeth and those with a mixture of teeth and bone.

[43] Temperature differences between Hole 913B and the ACEX sites would have been much too small to explain the large difference in $\delta^{18}O$. It is possible that the salinity at Hole 913B, which was located in close proximity to land according to the high C/N ratios at the site [*Andreasson et al.*, 1996], was influenced by a nearby freshwater outflow. The paleodepth of Hole 913B is uncertain because of the unknown nature of the basement, but it is also possible that the site could have been quite shallow during the early Eocene and that the isotopic composition of the fish debris undergoing alteration at the sediment-water interface might more fully record the extent of freshwater episodes than the ACEX Sites, which, at a paleodepth of a few hundred meters, may have been below the mixed layer.

[44] Alternatively, it is possible that salinities of the Greenland Basin were actually lower than those of the Arctic during the early Eocene. *Andreasson et al.* [1996] argue that in the early Eocene the Greenland Basin was isolated with a very large drainage area to basin area ratio according to paleogeographic reconstructions. *Brinkhuis et al.* [2006] correlated the ACEX and Hole 913B cores, assigning an age of ~49.3 Ma to the base of Core 50R and placing the termination of the *Azolla* event at the top of Core 47R. Thus, many of the Hole 913B samples examined by *Andreasson et al.* [1996] actually correspond to a period when low sea level and relative isolation may have driven salinities to extreme lows, although samples taken from Hole 913 B after the *Azolla* event also show very low $\delta^{18}O$ values. *Brinkhuis et al.* [2006] hypothesize that freshwater outflows from the Arctic were a source of *Azolla* remains to the sediments of the nearby Nordic Seas, but the results from the Hole 913B samples indicate that the waters of the Norwegian Greenland Sea could have actually been as fresh or fresher than the Arctic Ocean during the early Eocene.

8. Conclusions

[45] Salinity reconstructions using fish bone $\delta^{18}O_{CO3}{}^{2-}$ reveal that the Arctic Ocean was probably brackish during most of the early and early middle Eocene, with an average salinity of 21 to 25‰, as compared to ~35‰ at ~18 Ma. During much of this period, a shallow water connection probably existed between the Arctic Ocean and the North Atlantic, and therefore the formation of deep and intermediate water in the North Atlantic may have been affected by the outflow of brackish water from the Arctic. Three negative excursions occur in the $\delta^{18}O_{CO3}{}^{2-}$ record, marking the PETM, the *Azolla*, and 47.6 Ma events. The salinity range reconstructed for the PETM of ~17–24‰ indicates that salinities may have been below the Eocene average, but extreme warmth may account for most of the negative excursion in $\delta^{18}O_{CO3}{}^{2-}$ during this event. It is possible that the Arctic was isolated from the North Atlantic during the PETM, as *Knox* [1998] reports mammal migrations between North America and Europe across the Greenland-Faroe Ridge. However, the Arctic probably maintained a shallow water connection to the world ocean through the Turgay Strait at this time, so it is likely that low salinities would have developed from conditions of increased regional precipitation and runoff associated with extreme high-latitude warmth. The extent of freshening in the Arctic at the PETM is probably not fully recorded in our reconstruction because the samples examined in this study are not from the

interval in which *Pagani et al.* [2006] record the highest δD values.

[46] The lowest salinities obtained in this study correspond to the other two negative excursions in the $\delta^{18}O_{CO3}{}^{2-}$ record: the *Azolla* event reported by *Brinkhuis et al.* [2006] at ~48.7 Ma and a previously unidentified event at ~47.6 Ma. Both of these events probably correspond to sea level lowerings of 20–30 m reported by *Miller et al.* [2005b] and occur after connections through the Turgay Strait had ceased at 49 Ma [*Radionova and Khokhlova*, 2000]. The salinity range of 16 to 21‰ obtained for these events is probably not low enough to support the growth of *Azolla* in open waters. However, it is possible that the bones were altered to reflect conditions at the sediment-water interface at a depth of a few hundred meters, and that, except in brief seasonal floods, the salinities obtained in this study do not reflect the full extent of freshening in surface waters, but rather provide an upper bound on surface water salinity.

[47] **Acknowledgments.** Samples were provided by the Integrated Ocean Drilling Program (IODP), which is sponsored by the U.S. National Science Foundation (NSF) and other participating countries. Funding for this research was provided by the U.S. Science Support Program of the Joint Oceanographic Institutions. We wish to thank our reviewers Paul Wilson and Clive Trueman for valuable comments on the manuscript; Lora Wingate of the University of Michigan Stable Isotope Laboratory for the carbonate analyses; James Gleason for valuable collaborations; Joanne Reuss, Sarah Bradbury, Jenny Kucera, and Shih-Yu Lee for laboratory support; Wenjun Yong for assistance with the SEM; Gerry Smith, Appy Sluijs, Catherine Stickley, and Paul Koch for helpful discussions; and K. C. Lohmann for helpful suggestions on the manuscript.

References

Aagaard, K., and E. C. Carmack (1989), The role of sea ice and other fresh water in the Arctic circulation, *J. Geophys. Res.*, *94*(C10), 14,485–14,498.

Andreasson, F. P., B. Schmitz, and D. Spiegler (1996), Stable isotopic composition ($\delta^{18}O_{CO3}{}^{2-}$ and $\delta^{13}C$) of early Eocene fish-apatite from Hole 913B: An indicator of the early Norwegian-Greenland Sea paleosalinity, *Proc. Ocean Drill. Program Sci. Results*, *151*, 583–591.

Averianov, A. O., and J. D. Archibald (2003), Mammals from the Upper Cretaceous Aitym Formation, Kyzylkum Desert, Uzbekistan, *Cretaceous Res.*, *24*, 171–191.

Backman, J., et al. (2008), Age model and core-seismic integration for the Cenozoic Arctic Coring Expedition sediments from the Lomonosov Ridge, *Paleoceanography*, doi:10.1029/2007PA001476, in press.

Bauch, D., P. Schlosser, and R. G. Fairbanks (1995), Freshwater balance and the sources of deep and bottom waters in the Arctic Ocean inferred from the distribution of $H_2^{18}O$, *Prog. Oceanogr.*, *35*, 53–80.

Bice, K. L., and J. Marotzke (2002), Could changing ocean circulation have destabilized methane hydrate at the Paleocene/Eocene boundary?, *Paleoceanography*, *17*(2), 1018, doi:10.1029/2001PA000678.

Bice, K. L., M. A. Arthur, and L. Marincovich Jr. (1996), Late Paleocene Arctic Ocean shallow-marine temperatures from mollusc stable isotopes, *Paleoceanography*, *11*(3), 241–249.

Brewer, P. G., W. S. Broecker, W. J. Jenkins, P. B. Rhines, C. G. Rooth, J. H. Swift, T. Takahashi, and R. T. Williams (1983), The climatic freshening of the deep Atlantic north of 50°N over the past 20 years, *Science*, *222*, 1237–1239.

Brinkhuis, H., et al. (2006), Episodic fresh surface water in the Eocene Arctic Ocean, *Nature*, *441*, 606–609.

Bukry, D. (1984), Paleogene paleoceanography of the Arctic Ocean is constrained by the middle or late Eocene age of USGS Core Fl-422: Evidence from silicoflagellates, *Geology*, *12*, 199–201.

Burke, W. H., R. E. Denison, E. A. Hetherington, H. F. Koepnick, H. F. Nelson, and J. B. Otto (1982), Variation of seawater $^{87}Sr/^{86}Sr$ throughout Phanerozoic time, *Geology*, *10*, 516–519.

Clark, D. C., and J. A. Kitchell (1979), Comment on "The terminal Cretaceous event: A geological problem with an oceanographic solution", *Geology*, *7*, 228.

Craig, H., and L. I. Gordon (1965), Deuterium and oxygen 18 variations in the ocean and the marine atmosphere, in *Stable Isotopes in Oceanographic Studies and Paleotemperatures*, edited by E. Tongiorgi, pp. 9–130, Lab. di Geol. Nucl., Pisa, Italy.

Dickens, G. R. (1999), The blast in the past, *Nature*, *401*, 752–755.

Estes, R., and J. H. Hutchinson (1980), Eocene lower vertebrates from Ellesmere Island, Canadian Arctic Archipelago, *Palaeogeogr. Palaeoclimatol. Palaeoecol.*, *30*, 325–347.

Expedition 302 Scientists (2005), *Preliminary Report: Paleoceanographic and Tectonic Evolution of the Central Arctic Ocean*, *Arctic Coring Expedition (ACEX), Integr. Ocean Drill. Program Prelim. Rep.*, *302*, doi:10.2204/iodp.pr.302.2005.

Expedition 302 Scientists (2006), Sites M0001–M0004, in *Arctic Coring Expedition (ACEX)*, *Proc. Integr. Ocean Drill. Program*, *302*, doi.10.2204/iodp.proc.302.104.2006.

Fairbanks, R. G., C. D. Charles, and J. D. Wright (1992), Origin of global meltwater pulses, in *Radiocarbon After Four Decades*, edited by R. E. Taylor, pp. 473–500, Springer, New York.

Friedman, I., and J. R. O'Neil (1977), Compilation of stable isotope fractionation factors of geochemical interest, in *U. S. Geol. Surv. Prof. Pap.*, *440-KK*.

Gradstein, F. M., and S. P. Srivastava (1980), Aspects of Cenozoic stratigraphy and paleoceanography of the Labrador Sea and Baffin Bay, *Palaeogeogr. Palaeoclimatol. Palaeoecol.*, *30*, 261–295.

Greenwood, D. R., and S. L. Wing (1995), Eocene continental climates and latitudinal temperature gradients, *Geology*, *23*, 1044–1048.

Hubert, J. F., P. T. Panish, D. J. Chure, and K. S. Prostak (1996), Chemistry, microstructure, petrology, and diagenetic model of Jurassic dinosaur bones, Dinosaur National Monument, Utah, *J. Sediment. Res.*, *66*(3), 531–547.

Iakovleva, A. I., H. Brinkhuis, and C. Cavagnetto (2001), Late Paleocene-early Eocene dinoflagellate cysts from the Turgay Strait, Kazakhstan; correlations across ancient seaways, *Palaeogeogr. Palaeoclimatol. Palaeoecol.*, *172*, 243–268.

Jahren, A. H., and L. S. L. Sternberg (2002), Eocene meridional weather patterns reflected in the oxygen isotopes of Arctic fossil wood, *GSA Today*, *12*(1), 4–9.

Jahren, A. H., and L. S. L. Sternberg (2003), Humidity estimate for the middle Eocene Arctic rain forest, *Geology*, *31*, 463–466.

Jakobsson, M., et al. (2007), The early Miocene onset of a ventilated circulation regime in the Arctic Ocean, *Nature*, *447*, 986–990.

Johnson, G. L., J. Pogrebitsky, and R. Macnab (1994), Arctic structural evolution: Relationship to paleoceanography, in *The Polar Oceans and Their Role in Shaping the Global Environment*, *Geophys. Monogr. Ser.*, vol. 85, edited by O. M. Johannessen, R. D. Muench, and J. E. Overland, pp. 285–294, AGU, Washington D. C.

Knox, R. W. O. (1998), The tectonic and volcanic history of the North Atlantic region during the Paleocene-Eocene transition: Implications for NW European and global biotic events, in *Late Paleocene-Early Eocene Climatic and Biotic Events in the Marine and Terrestrial Records*, edited by M. P. Aubry, S. G. Lucas, and W. A. Berggren, pp. 91–102, Columbia Univ. Press, New York.

Koch, P. L., N. Tuross, and M. L. Fogel (1997), The effects of sample treatment and diagenesis on the isotopic integrity of carbonate in biogenic hydroxylapatite, *J. Archaeol. Sci.*, *24*, 417–429.

Kohn, M. J., and J. M. Law (2006), Stable isotope chemistry of fossil bone as a new paleoclimate indicator, *Geochim. Cosmochim. Acta*, *70*, 931–946.

Kolodny, Y., and B. Luz Jr. (1991), Oxygen isotopes in phosphates of fossil fish—Devonian to Recent, in *Stable Isotope Geochemistry: A Tribute to Samuel Epstein*, edited by H. P. Taylor, J. R. O'Neil, and I. R. Kaplan, pp. 105–119, Geochem. Soc., San Antonio, Tex.

Kolodny, Y., B. Luz, M. Sander, and W. A. Clemens (1996), Dinosaur bones: Fossils or psuedomorphs? The pitfalls of physiology reconstruction from apatitic fossils, *Palaeogeogr. Palaeoclimatol. Palaeoecol.*, *126*, 161–171.

Lawver, L. A., R. D. Müller, S. P. Srivastava, and W. Roest (1990), The opening of the Arctic Ocean, in *Geological History of the Polar Oceans: Arctic Versus Antarctic*, edited by U. Bleil and J. Thiede, pp. 29–62, Kluwer Acad., Dordrecht, Netherlands.

Lawver, L. A., A. Grantz, and L. M. Gahagan (2002), Plate kinematic evolution of the present Arctic region since the Ordovician, in *Tectonic Evolution of the Bering Shelf–Chuckchi Sea–Arctic Margin and Adjacent Landmasses*, edited by E. L. Miller, A. Grantz, and S. L. Klemperer, pp. 333–358, Geol. Soc. of Am., Boulder, Colo.

Lear, C. H., H. Elderfield, and P. A. Wilson (2000), Cenozoic deep-sea temperatures and global ice volumes from Mg/Ca in benthic foraminiferal calcite, *Science*, *287*, 269–272.

Magavern, S., D. L. Clark, and S. L. Clark (1996), $^{87/86}$Sr, phytoplankton, and the nature of the Late Cretaceous and early Cenozoic Arctic Ocean, *Mar. Geol.*, *133*, 183–192.

Manabe, S. (1997), Early development in the study of greenhouse warming: The emergence of climate models, *Ambio*, *26*(1), 47–51.

Marincovich, L., Jr., E. M. Brouwers, D. M. Hopkins, and M. C. McKenna (1990), Late Mesozoic and Cenozoic paleogeographic and paleoclimatic history of the Arctic Ocean Basin, based on shallow-water marine faunas and terrestrial vertebrates, in *The Arctic Ocean Region*, edited by A. Grantz, L. Johnson, and J. F. Sweeney, pp. 403–406, Geological Soc. of Am., Boulder, Colo.

Meyers, P. A., and S. M. Bernasconi (2005), Carbon and nitrogen isotope excursions in mid-Pleistocene sapropels from the Tyrrhenian Basin: Evidence for climate-induced increase in microbial primary production, *Mar. Geol.*, *220*, 41–58.

Miller, K. G., M. A. Kominz, J. V. Browning, J. D. Wright, G. S. Mountain, M. E. Katz, P. J. Sugarman, B. S. Cramer, N. Christie-Blick, and S. F. Pekar (2005a), The Phanerozoic record of global sea-level change, *Science*, *310*, 1293–1298.

Miller, K. G., J. D. Wright, and J. V. Browning (2005b), Visions of ice sheets in a greenhouse world, *Mar. Geol.*, *217*, 215–231.

Moore, T. C., and Expedition 302 Scientists (2006), Sedimentation and subsidence history of the Lomonosov Ridge, in *Arctic Coring Expedition (ACEX)*, *Proc. Integr. Ocean Drill. Program*, *302*, doi:10.2204/iodp.proc.302.105.2006.

Moran, K., et al. (2006), The Cenozoic palaeoenvironment of the Arctic Ocean, *Nature*, *441*, 601–605.

Moriya, K., P. A. Wilson, O. Friedrich, J. Erbacher, and H. Kawahata (2007), Testing for ice sheets during the mid-Cretaceous greenhouse using glassy foraminiferal calcite from the mid-Cenomanian tropics on the Demerara Rise, *Geology*, *35*, 615–618.

Mueller-Lupp, T., H. Erlenkueser, and H. A. Bauch (2003), Seasonal and interannual variability of Siberian river discharge in the Laptev Sea inferred from stable isotopes in modern bivalves, *Boreas*, *32*, 292–303.

Nunes, F., and R. D. Norris (2006), Abrupt reversal in ocean overturning during the Palaeocene/Eocene warm period, *Nature*, *439*, 60–63.

Onodera, J., K. Takahashi, and R. W. Jordan (2007), Eocene silicoflagellate and ebridian paleoceanography in the central Arctic Ocean, *Paleoceanography*, PA1S15, doi:10.1029/2007PA001474.

Pagani, M., et al. (2006), Arctic hydrology during global warming at the Paleocene/Eocene thermal maximum, *Nature*, *442*, 671–675.

Radionova, E. P., and I. E. Khokhlova (2000), Was the North Atlantic connected with the Tethys via the Arctic in the early Eocene? Evidence from siliceous plankton, *GFF*, *122*, 133–134.

Scheurle, C., and D. Hebbeln (2003), Stable oxygen isotopes as recorders of salinity and river discharge in the German Bight, North Sea, *Geo Mar. Lett.*, *23*, 130–136.

Sluijs, A., et al. (2006), Subtropical Arctic Ocean temperatures during the Paleocene/Eocene thermal maximum, *Nature*, *441*, 610–613.

Srivastava, S. P. (1985), Evolution of the Eurasian basin and its implications to the motion of Greenland along Nares Strait, *Tectonophysics*, *114*, 29–53.

Stickley, C., N. Koç, H.-J. Brumsack, R. W. Jordan, and I. Suto (2008), A siliceous microfossil view of middle Eocene Arctic paleoenvironments: A window of biosilica production and preservation, *Paleoceanography*, doi:10.1029/2007PA001485, in press.

St. John, K., and D. Willard (2006), Cenozoic (0–46 Ma) ice-rafting history of the central Arctic: Terrigenous sands on the Lomonosov Ridge, *Eos Trans. AGU*, *87*(52), Fall Meet. Suppl., Abstract U24A-07.

Thiede, J., and A. M. Myhre (1996), Introduction to the North Atlantic-Arctic gateways: Plate tectonic-paleoceanographic history and significance, *Proc. Ocean Drill. Program Sci. Results*, *151*, 3–23.

Toyoda, K., and M. Tokonami (1990), Diffusion of rare-earth elements in fish teeth from deep-sea sediments, *Nature*, *345*, 607–609.

Tripati, A., J. Zachos, L. Marincovich Jr., and K. L. Bice (2001), Late Paleocene Arctic coastal climate inferred from molluscan stable and radiogenic isotope ratios, *Palaeogeogr. Palaeoclimatol. Palaeoecol.*, *170*, 101–113.

Trueman, C. N., and N. Tuross (2002), Trace elements in recent and fossil bone apatite, *Rev. Mineral. Geochem.*, *48*, 489–521.

Trueman, C. N., A. K. Behrensmeyer, R. Potts, and N. Tuross (2006), High-resolution records of location and stratigraphic provenance from the rare earth element composition of fossil bones, *Geochim. Cosmochim. Acta*, *70*, 4343–4355.

Vetshteyn, V. Y., G. A. Malyuk, and V. P. Rusanov (1974), Oxygen-18 distribution in the central Arctic Basin, *Oceanology*, *14*(4), 514–519.

Wright, J. D. (1998), Role of the Greenland-Scotland Ridge in Neogene climate changes, in *Tectonic Boundary Conditions for Climate Reconstructions*, edited by T. J. Crowley and K. C. Burke, pp. 192–211, Oxford Univ. Press, Oxford, U. K.

Zachos, J., L. D. Stott, and K. C. Lohmann (1994), Evolution of early Cenozoic marine temperatures, *Paleoceanography*, *9*(2), 353–387.

Zachos, J., M. Pagani, L. Sloan, E. Thomas, and K. Billups (2001), Trends, rhythms, and aberrations in global climate 65 Ma to present, *Science*, *292*, 686–693.

Zahn, R., and A. C. Mix (1991), Benthic foraminiferal δ^{18}O in the ocean's temperature-salinity-density field: Constraints on ice age thermohaline circulation, *Paleoceanography*, *6*(1), 1–20.

Zazzo, A., C. Lécuyer, and A. Mariotti (2004), Experimentally-controlled carbon and oxygen isotope exchange between bioapatites and water under inorganic and microbially-mediated conditions, *Geochim. Cosmochim. Acta*, *68*, 1–12.

T. C. Moore and L. M. Waddell, Department of Geological Sciences, University of Michigan, 2534 C. C. Little Building, 1100 North University Avenue, Ann Arbor, MI 48109-1005, USA. (waddelin@umich.edu)